Imaging the TRINAT Trap

TRIUMF Summer Work Term Report

Erin Broatch

August 25th, 2017

Contents

1 Background

1.1 Magneto-Optical Trap and Optical Pumping

Because the TRINAT experiments require cooled *and* well-polarized atoms, we need to use a two-part cycle of trapping and optical pumping. Much of the work summarized in this report involves the optical pumping (polarization) part of the cycle. If the optical pumping is successful, the polarized atoms should stop fluorescing. The brightness of the cloud before and after the polarizing period can therefore be used to evaluate the quality of the atom's polarization. Also note that the trap light and optical pumping light are at slightly different wavelengths: 767nm and 770nm, respectively.

1.2 Motivation for Improved Imaging

Photographing the trap can allow us to study several properties, such as the trap lifetime, cloudshape, and quality of polarization. Moving towards higher light sensitivity and stronger signals in our images will allow useful images to be captured even with lower quantities of atoms in the trap, such as when running the experiment with radioactives. Enabling higher bit-depth imaging also allows us to resolve features in low-brightness images. In addition, characterizing the timing performance of the camera allows for the possibility of using shorter exposure times with more accurate timing of photos.

2 CMOS Camera and Settings

2.1 Description of Camera Technology

The core element of a digital camera is its sensor, which is composed of thousands or millions of pixels. Each pixel converts light into electrons via the photoelectric effect and the sensor subsequently reads these charges into a digital image. Several quantities can be used to characterize a sensor's properties:

- Quantum Efficiency [%]: what percentage of incident photons create electrons (depends on wavelength)
- Saturation Capacity [e-]: the maximum number of electrons that can be stored in the pixel's potential well
- Pixel Size [μm]: physical dimensions of the pixel
- ADC: how many bits are used in the analog (charge) to digital (greyscale) conversion

A more in-depth treatment of the factors affecting camera sensitivity can be found in Point Grey's Article "How to Evaluate Camera Sensitivity" [6].

2.2 CMOS vs CCD

There are two main categories of digital camera sensors, each with its own advantages and disadvantages. The traditional sensor is the charge-coupled device (CCD). A CCD sensor has only one (or at most, a handful of) amplifiers to read off the charge. As a result, electrons must be moved across the sensor so that they can be read sequentially by the amplifier. By changing the voltages applied to the potential wells, charges can be shifted down the sensor one row at a time until they reach the bottom where the amplifier is located.

The primary advantage of CCD cameras is their low noise and high light sensitivity, which makes them optimal for astrophotography and similar situations. As well, all CCD cameras offer a global shutter, meaning that all pixels are exposed to capture the same period of time. However, because of the nature of the CCD architecture, the manufacturing process is much more specialized, which also leads to high costs. As well, the vertical channels which allow electrons to be moved down the sensor can also lead to oversaturated parts of the image spilling over to neighbouring pixels (blooming) and causing bright vertical stripes in the image.

Meanwhile, complementary metal-oxide-semiconductor (CMOS) sensors contain an amplifier for each individual pixel. This means that the signal is digitized at the pixel. However, the amplifier takes up some of the space on the pixel, reducing the light sensitive area. The CMOS sensors, while compromising light sensitivity, offer other advantages, notably lower costs, no blooming and low power consumption (up to 100 times less than CCD). Certain CMOS cameras use a rolling shutter, meaning that each row of the image is exposed at a slightly different time, which can lead to artifacts. However, other CMOS cameras have a global shutter similar to a CCD.

The sensor in our newly implemented Grasshopper3 camera is the Sony Pregius IMX252. This is a CMOS sensor but with some elements of CCD giving global shutter and low noise.

2.3 Camera Characterization

The new camera that we have implemented from Point Grey is the Grasshopper3 (referred to here as GS3.) The GS3 has high quantum efficiency in the near-IR region and a 12-bit ADC. Further specifications can be found in the Grasshopper3 Datasheet [4], Technical Reference [3], and Imaging Performance Specification [2] documents.

Linearity

The integrated intensity (sum of pixel values) for images taken at different exposure lengths were graphed to determine the linearity of the camera's response. An externally powered LED light was used to illuminate the camera. We would expect that as the camera is exposed to the light for longer times, the total brightness should increase proportionally. Fig 2.3 below shows the results of a

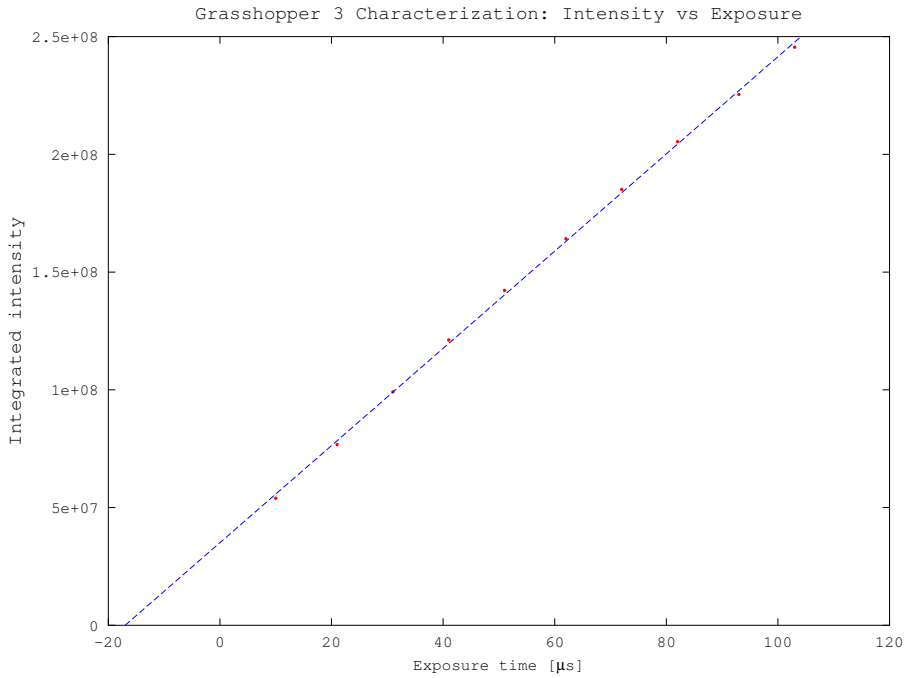

Figure 1: Integrated intensity (sum of pixel values) for varying exposure lengths for the Grasshopper3 camera. The intensity increases quite linearly with exposure time. Note the positive y-intercept and x-intercept at -16.985μs. This may have been caused by the brightness register which adds a constant offset to each pixel.

test to characterize the linearity. Note that the exposure length can only be set to certain discrete values. If you attempt to set the camera to a different exposure length than one of these allowed values, it will automatically be set to the nearest allowed value. Also note that the brightness register, only discovered later on, may account for some to the vertical offset in these images.

Timing

The timing of the image relative to the trigger can be determined from several methods. The first was to use a pulsed LED powered by a function generator. The camera trigger signal could also be used to trigger the LED signal. The delay on the start of the LED pulse relative to the camera trigger was varied. The LED pulse is the same length as the exposure. Therefore, when the LED starts at the same time as the camera exposure, the two will be completely overlapped and the integrated intensity should be at its highest. The results of a characterization test similar to that described above can be seen in Figure 2.3.

Using this method, the timing delay was estimated to be $\sim 32\mu$s. The plateau seen in Figure 2.3 is not expected.

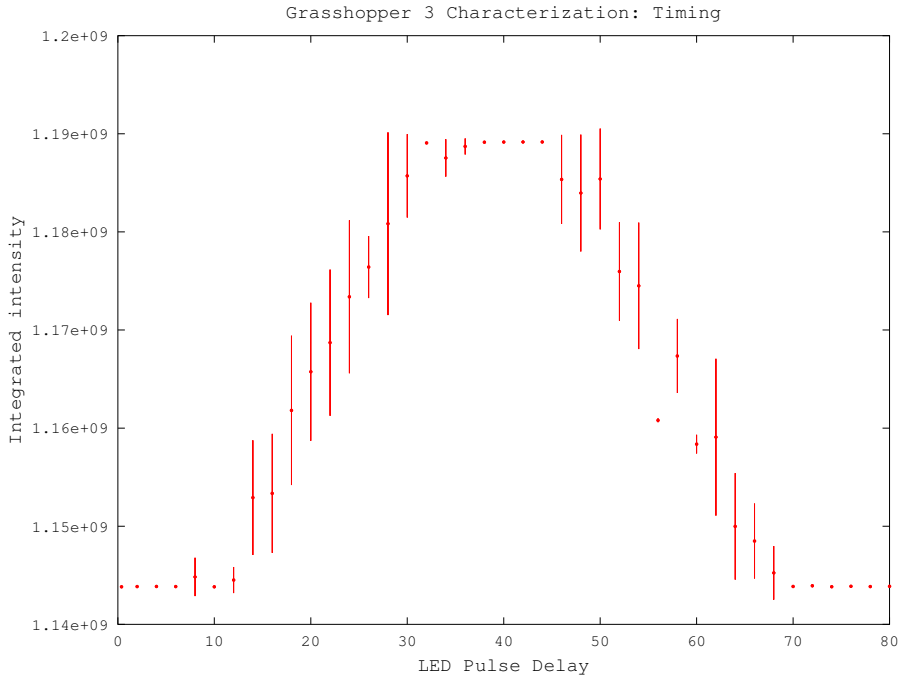

Figure 2: Results of the LED pulse timing test. An exposure time of 21μs was used with an LED pulse of 21μs. The LED pulse was started with varying delays from the camera triggering time. The images should reach their maximum intensity when the LED pulse and camera integration begin at the same time. Therefore, from this graph with estimate the timing delay of the camera integration to be $\sim 32\mu$s

Another method for characterizing the timing delay was discovered later through the camera strobe settings. The strobe signal can be configured to fire either on the trigger or at the start of integration. By setting the strobe to fire at the start of integration, we can directly compare the delay between the trigger signal and the strobe signal on a digital scope. Using this method, the timing delay was found to vary between 18μs and 25μs.

Firefly, Flea 13Y3M and Flea 13E4M

Before the Grasshopper was implemented, similar linearity and timing characterizations were performed for the Firefly, Flea 13Y3M and Flea 13E4M cameras. However, there were several effects with then-unknown causes, such as significant vertical offsets in the linearity plots and changing backgrounds. While we

initially attributed this to erratic dark current properties, I now believe that many of these problems were caused by an auto-adjusting brightness register, which adds an offset onto all the greyscale pixel values in an image. In the current camera codes this brightness register has been set to zero with no auto-adjust which should resolve the issue. The Grasshopper3 is a very good camera with overall better specifications than the Firefly and Flea 13Y3M and 13E4M, however I do not doubt that these three cameras can still find a suitable use in the lab now that their settings and properties are more well-understood.

2.4 Registers and Settings

The Grasshopper3 camera, as well as the Firefly and Flea cameras, all have emphregisters which are used to inquire or apply various settings. These can be adjusted either through the flycap GUI program settings menu, manually through the flycap GUI settings "Registers" tab, or in the C++ code currently used to control the camera and synchronize with the trap. To ensure consistency between images, certain settings should NOT be set to automatic-adjustment mode.

A complete documentation of available registers can be found in the FLIR Digital Camera Register Reference [1]. However, the most important settings to be aware of for our purposes are:

- Format 7 Mode: MODE_7 produces 12-bit images
- Shutter: The shutter value, or exposure length, measures how long the camera integrates an image for. Only certain discrete values are allowed (for the GS3 with a full image in 16-bit these are 10μs, 21 μs, 31μs, 41μs, 51μs, 62μs, 72μs, etc). The smallest exposure value of 5μs is allowed with a smaller region of interest (ROI). The shutter/exposure length should NOT be auto-adjusted.
- Gain: The gain is a multiplication factor for the greyscale value of the pixels. This should be set to 0.0 and NOT auto-adjusted.
- Brightness: The brightness is a constant offset added onto all the pixel values in an image. Before we discovered this register, a constant offset applied to images led to much confusion regarding the linearity and time response of the cameras. All this to say that the brightness should also be set to 0.0 and NOT auto-adjusted.
- Trigger Mode Source: A source value of 0 allows a software trigger to be used, while a source value of 7 configures the camera for external hardware triggering.
- Trigger Mode Polarity: Can be set to 0 for active low (falling-edge) or 1 for active high (rising edge).
- Strobe Polarity: Set in the same way as the trigger mode polarity.

- GPIO_XTRA: This register (0x1104) controls whether the strobe output fires at the same time as the trigger, or at the start of integration. Setting this to the start of integration allows the delay between the trigger and the actual exposure to be determined (using a scope to compare the two signals, for example).

There are many other input parameters for the camera which can be modified by accessing the proper registers. Appendix D in the Grasshopper3 Technical Reference [3] is a useful resource detailing the available control and status registers. In addition, the CustomImageEx2.cpp code allows for several commonly varied settings (exposure time, and the location of a region of interest smaller than the maximum image size) to be modified via a text file called camparam.txt rather than in the camera code itself (see Section 4.3 for further detail).

2.5 Hardware Setup

Because the Grasshopper3 does not have any controls on the camera, it must be controlled from an external source. There are two connections to the camera: the first is a USB cable, and the second is a general-purpose-input-output (GPIO) cable with 8 internal wires. The USB cable is used to connect to the laptop (White Samsung behr@behrsam1) which runs the camera and stores the photos. The GPIO cable serves several purposes. Most importantly, it powers the camera (note that the GS3 has a higher power consumption, up tp 4.5W, so it is possible but unwise to power it from the laptop through the USB). The GPIO cable also allows external trigger signals from the Pi to be sent to the camera, allowing the timing of the images to be synchronized to the trap sequence.

Finally, the camera outputs a strobe signal which is sent via the GPIO cable back to the Pi to indicate that a picture has been taken. I have changed the camera settings so that the strobe will fire at the start of integration instead of on the trigger. Using this feature, we observe that the delay between the trigger and the start of integration ranges between 18μs and 25μs.

For the strobe to output a strong enough signal to be detected by the Pi, a pull-down resistor and battery circuit is required - see Claire Preston's April report (Fig 2.3) for further details. As well, it was found that the rise time for the strobe signal is approximately 100μs. The strobe from an exposure less than 50μs in length may not reach a high enough voltage to be detected by the Pi.

3 Optics

3.1 Objectives

With the GS3 camera in place and capable of capturing useable images of the trap, the next step was to improve the image quality and signal-to-noise ratio through the use of appropriate optics. Two complementary goals were prioritized in the design of a new optics stack: total light collection and magnification.

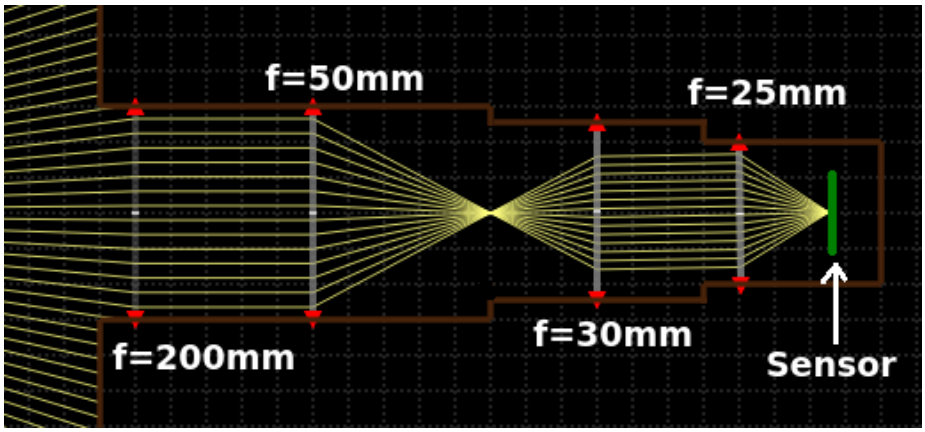

Figure 3: Ray diagram showing the idealized lens system. Grid boxes represent 5mm vertically and 10mm horizontally. Simulation created with Ray Optics Simulator (https://ricktu288.github.io/ray-optics/)

By increasing the amount of light initially collected from the trap and reducing losses along the length of the lens tube, more photons would hit the camera's CMOS sensor, thereby producing a stronger image. Using a magnification which makes the image of the trap on the sensor smaller also brightens the signal.

3.2 Design and Components

Lenses

Four achromatic lenses were used, with focal lengths and diameters as shown in Table 1 below. The back focal length (bfl) is the distance from the planar side of the lens to the focal point. A ray diagram simulation, showing the idealized lens system with thin lens equations, can be seen in Figure 3.2.

Table 1: Lenses used in the new optics stack. Lens 1 is closest to the trap and Lens 4 is closest to the camera.

lens	f [mm]	bfl [mm]	⌀[mm]
1	200	196.57	30
2	50	42.9	30
3	30	21.96	25
4	25	18.71	20

The larger diameter of lenses 1 and 2 allowed for increased light collection. The shorter focal length of lens 1 also increases light collection, as a larger solid angle is intercepted. The light collection is proportional to the solid angle (here approximated for small angles):

$$light\ collection \sim \Omega \approx \left(\frac{\varnothing_1}{f_1}\right)^2 \tag{1}$$

where Ω is the intercepted solid angle, $\varnothing_1$ is the diameter of the first lens and f_1 is the focal length of the first lens. Meanwhile, the total magnification of the system can be calculated using the formula

$$magnification = \frac{f_2 f_4}{f_1 f_3} \tag{2}$$

where f_1, f_2, f_3, f_4 represent the focals lengths of the first, second, third and fourth lenses, respectively (see Table 1). This leads to a magnification of 5/24, or $\sim$0.208 times. Given the light collection and the magnification, we know that the spot intensity should be proportional as follows:

$$spot\ intensity \sim \frac{light\ collection}{magnification^2} = \left(\frac{\varnothing_1 f_3}{f_2 f_4}\right)^2 \tag{3}$$

We finally achieve a relative spot intensity of 0.52 for the new system, as compared to 0.69 for the older system. A higher spot intensity could be achieved if a f=20mm,$\varnothing$=20mm achromat were available for use as the last lens. Unfortunately, we were not able to find such a lens with a near-IR coating. However, the important figure of merit here is that the overall light collection has been increased by a factor of 1.44.

Spherical Aberration

Why use achromatic lenses, especially when dealing with essentially monochromatic light? Initially, we purchased several plano-convex and biconvex lenses with identical focal lengths which should have fulfilled the same role. However, upon closer inspection it was discovered that the spherical aberration due to these lenses would be intolerable, degrading the image more than it could be improved. For lenses with long focal lengths compared to their diameter, thin lens equations are acceptable and spherical aberration can safely be ignored. In the case of lenses with similar focal lengths and diameters however, the lenses are decidedly not thin, and spherical aberration can have a large effect on the final image. The spot size (this is the size of the image for a point-like object) can be calculated using the formula

$$A = \frac{k y^4}{f^3} \tag{4}$$

$$D = \frac{8\ \Sigma A v}{y_f} \tag{5}$$

where A is the wavefront aberration for a single lens, k is a constant dependent on the orientation and type of lens (e.g. 0.0685 for plano-convex with the convex side facing a collimated beam), y is the semi-aperture or the maximum ray height from an on-axis object, y_f is the semi-aperture for the final lens, f is the focal length of the lens, D is the spot size caused by a set of lenses, and v is the distance between the final lens and the image [5]. Using plano-convex lenses for lens 1, 2, and 3, and a biconvex lens for lens 4, with the same diameters and focal lengths described in Table 1, this would result in a spot size (blur) of 1.94mm. Assuming a cloud diameter of 2mm, which would result in an image on the sensor of $\sim$0.4mm, this means that the spot size (blur) would be larger than the image of the trap itself, and as such would greatly restrict the quality of our images.

Filters and Aperture

A finely-adjustable aperture (iris) was placed near the focal point between lenses 2 and 3. By closing down this aperture just enough without clipping the image, more scattered light can be rejected. However, since the aperture is not located at exactly the focal point, it can not be turned down all the way. In a similar vein, a red glass filter (695nm) was placed between lenses 3 and 4, eliminating room lights.

An interference filter (Semrock LL01-780) was also placed in the stack to reject the trap light. The filter was angled so that 770nm (OP) light can pass through while 767nm (MOT) light is blocked. This helped to eliminate some persistent backgrounds from the trap light which remained even during the OP images when the trap was off. This mysterious background disappeared when there were no atoms in the trap. However, even with three different methods of trying to reduce the presence of the trap light during the optical pumping time (using an electro-optic switch and polarizer to reduce the detection of trap light by a factor of 30, turning the collection (first) trap light completely off, and turning off the push beam AOM's), the background remained. These backgrounds may be due to properties of the camera sensor itself, for example if a ghost image of the brighter trap image remains on the sensor for several milliseconds after it is exposed. (Hopefully we are not hurting the OP with MOT light). The consequence here is that the GS3 camera can no longer be used to take pictures of the trap to determine the number of atoms present. This function may require a second camera in the future.

3.3 Final Optics Stack

The completed optics stack is shown in Figure 3.3. Correct spacing between all of the elements in the lens assembly is incredibly important to ensure proper focusing and magnification of the image.

Cameras are equipped with various different systems for mounting lenses and other optics. The GS3 camera uses the C-mount standard, which has 1-32 UN 2A screw threads and a 0.69" (17.526mm) flange-focal-distance (FFD). To

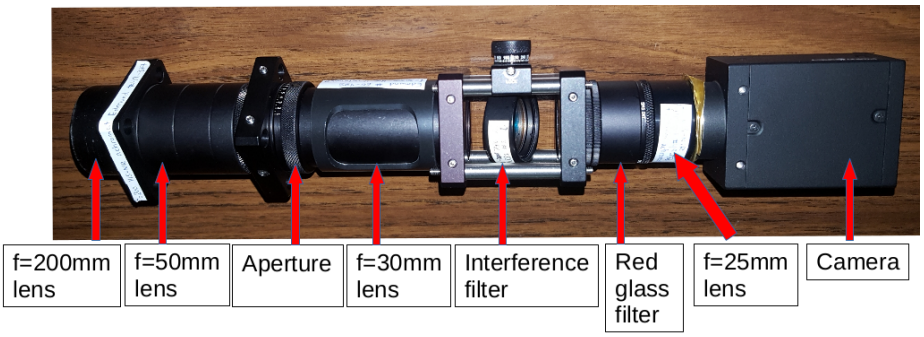

Figure 4: The assembled optics stack installed on the Grasshopper3 camera

obtain a focused image, the final lens (assuming parallel incoming light) must be located exactly at its focal length from the sensor. This was a challenge for us because using a C-mount to SM1 adapter would not allow a lens to be placed close enough to the sensor, while a C-mount lens holder will not accept ⌀1" optics, and otherwise holds the lens too close. We settled on a special ⌀20mm C-mount holder from Edmund Optics. However, this holds the lens too close to the sensor, so three vinyl spacers (0.030" thickness each) were made to sit inside the mount. (These were cut from a corner of the clean room door, how exciting!) Furthermore, a 2mm brass spacer and three thin brass shims were used over the C-mount threads to give the correct spacing.

The GS3 camera is located on the bottom viewport, looking up at the trap at 35 degrees. Therefore, it must be secured onto the viewport with an aluminum viewport mount. A previous mount, which was designed to hold 1" lens tubes, was modified by the TRIUMF machine shop to accept a 30mm lens tube. Additionally, a 30mm cage plate was installed as a flange to allow the optics stack to be reproducibly positioned with 1mm from the viewport itself. (This is what John Behr refers to as the "viewport non-smasher", do not remove it!)

The lens closest to the trap (lens 1, ⌀30mm, f=25mm) must be at a distance of one focal length from the trap itself. The distance from the viewport to the centre of the vacuum chamber (assumed to be the location of the trap) is 8"=203.2mm. Therefore the first lens should be placed as close to the viewport as possible without touching it. The distance between lens 1 and lens 2, as well as the distance between lens 3 and lens 4, need not be set precisely as the light is assumed to be parallel in those areas. To achieve optimum focusing, the distance between lens 2 and lens 3 must be carefully adjusted. Ideally, the spacing between the lenses need to be the sum of their back focal lengths. However, because the back focal length of the first light collection lens is 196.57mm and the cloud is slightly farther than the focal length, the spacing will differ slightly from the ideal value. To facilitate fine-tuned adjustment, lens 3 is housed in a slotted lens tube, so its position can be adjusted without disassembling the lens stack. Two empty 30mm lens tubes, a 30mm to 25.4mm adapter, and an empty

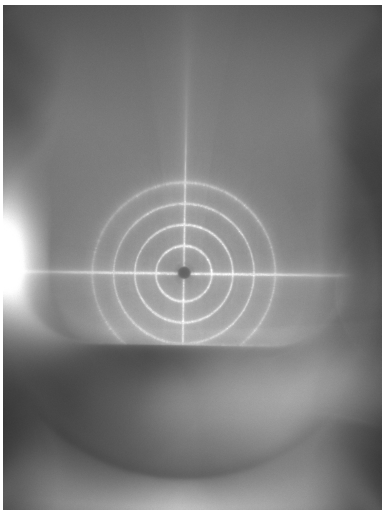

Figure 5: Size calibration image for the Grasshopper3 camera and optics. The Thorlabs alignment target pictured has rings with 4mm, 7mm, 10mm and 13mm diameter and the total image is 1536 by 2048 pixels. Therefore the size calibration is approximately 57.3pixels/mm

25.4mm lens tube are used as spacers. A C-mount to SM1 (Thorlabs thread) adapter is used between the lens 3 and lens 4.

One final consideration is that the optics need to be kept well-aligned to avoid any unwanted aberrations or defocus. Because the optics stack and camera is hanging from the viewport unsupported, this may induce unwanted deflection. In the future it may be beneficial to add a support for the camera and optics.

3.4 Image size calibration

During the focusing process a Thorlabs alignment target was placed at the same distance away from the camera as the cloud will be located when the optics are installed on the viewport. This also allowed us to capture several size calibration image (Figure 3.4) which will allow the size of the cloud to be determined in future tests. The rings on the alignment guide have diameters of 4mm, 7mm, 10mm, and 13mm. The dimensions of a full image from the Grasshopper3 is 2048 by 1536 pixels, and the largest ring measures approximately 745 pixels in diameter. This leads to an image size calibration of $\sim$57.3 pixels/mm.

4 Trap and Camera Triggering Cycle

4.1 Overview

The trap and camera triggering cycle is controlled by several interacting systems. The trap settings and timing is controlled by the Raspberry Pi in conjunction with several function generators and logic boxes. More information regarding this setup is available in Liam Lawrence's co-op report. The camera is being operated by another computer, behrsam1. However, at select times during the trap cycle, the Pi outputs a logic signal which is used as a hardware trigger for the camera, and the camera outputs strobes during the integration period which are sent back to the Pi to notify it that the picture has been taken.

4.2 Pi Code

There are many different trap sequences on the Pi that can be used to run the trap. The most recent incarnation that we have been using is TrapSeq_cp3_RAC_cloudshape_1period_OPbkg_longpush_Trap1off. In this version of the sequence, atoms are pushed 10 times per cycle before the optical pumping period. This leads to more atoms in the trap and brighter images. As well, the light in the collection (first) trap is turned of during the optical pumping period.

4.3 Camera Code

The GS3 camera is run from the white Samsung laptop behr@behrsam1 (connect remotely via behr@behrch1). The camera code can be found in the folder behr/pointgrey/flycapture2-2.11.3.121-amd64/src/CustomImageEx and run using the command `./CustomImageEx2`. The CustomImageEx2 program sets up the GS3 camera to use appropriate settings (such as no automatic adjustment of exposure length, no brightness offset, etc) for capturing images of the trap. It also configures the camera to accept hardware triggers via the GPIO pin and to output strobe signals also via the GPIO pins, As well, the camera captures a given number of images and writes each image as a 16-bit monochrome .png file into the same CustomImageEx folder before exiting. The image files are named in ascending order as pic-0,pic-1,pic-2, etc. It is important to note that the camera will essentially blindly accept triggers coming from the Pi. Therefore, the CustomImageEx2 program should be started before the Pi code in the interest of synchronization. Also, be wary of the fact that if the camera misses a trigger at some point (possible if the region of interest is too large or if exposures are too long) then the sequence of images will be incorrect.

The advantage of the CustomImageEx2 program over CustomImageEx is that it can take inputs from a text file called camparam.txt. This allows settings to be changed more easily and eliminates the need to recompile the program. The number of images, exposure length, and location of the region of interest can be controlled through this file. (Note however that the CustomImageEx2

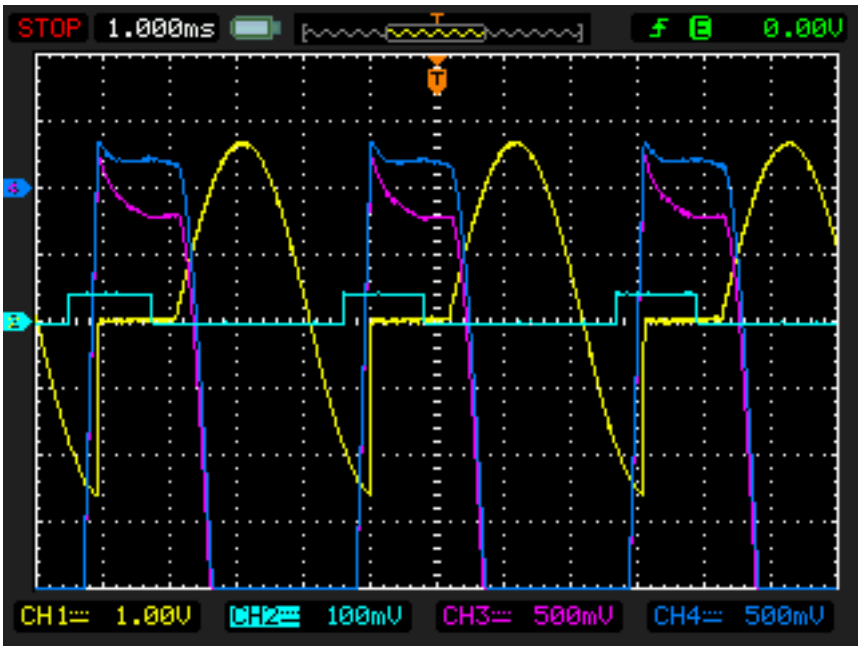

Figure 6: Screen capture of oscilloscope displaying bias magnetic field currents in pink and blue, and one of the voltage-control signals for the current in one of the coils in green. The coils are well-balanced towards the end of the optical pumping period.

has not yet been tested with the camera so I cannot guarantee that the text input will work.) The current region of interest that I have been using is 768 by 768 pixels, centered within the full sensor dimensions. Further reductions to the region of interest can also be applied during the image processing stage in Octave.

4.4 Function generators

We also implemented new BK precision function generators to control the bias magnetic fields and EOM's. Each coil for the bias magnetic field has its own channel on the function generator which improved the balancing of the currents. Settings can be found in my logbook on page 82. Additional settings can be found on page 59. An image of the oscilloscope in Figure 6 shows that the currents are fairly well-balanced around zero towards the end of the optical pumping period but a significant overshoot affects the balancing at the beginning of the optical pumping period.

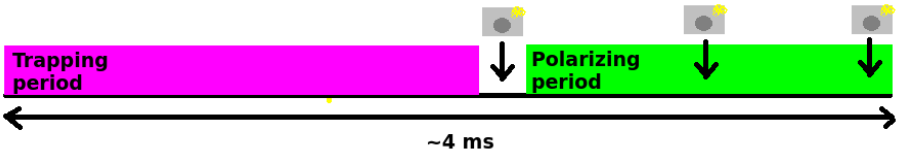

Figure 7: Timing diagram sketch for images taken during the trim field scan. Not to scale.

5 Magnetic Field Current Optimization

5.1 Trim Magnetic Field Scan

It is extremely important to have precisely set magnetic fields within the vacuum chamber. To this end, trim coils located on the outside of the vacuum chamber and on the rectangular frames are used to cancel out the fields from the cyclotron (when ON) and the earth's magnetic field. To optimize the magnetic fields from these two sets of coils, we scanned the currents around the historical "best value" and used the images from the Grasshopper3 camera to determine a new optimum setting. Three images were taken during the cycle: one in the short period after the MOT is turned off and before the optical pumping begins, one in the middle of the optical pumping period, and one at the end. Because the atoms should fluoresce less as they become more well-polarized, we would expect the pictures to decrease in their intensity throughout the optical pumping time. Therefore, a comparison of the second image and third images to the first bright image should reflect the degree of success of our attempts at polarization. Note that the bias magnetic field current waveforms (shown in Figure 6) are not well balanced near the start of the optical pumping period which may affect the second image.

5.2 Results

For each current value scanned, 10 images were captured and summed from each of the optical pumping peak, mid-optical pumping period and end of optical pumping period. A gaussian curve with a constant offset was fit to the projection of each picture onto the horizontal axis (see Appendix A.3 for more detail). The area (normalization factor) for these curves was taken to represent the brightness of the image. The tail-to-peak ratio, which is the area of the second or third composite image normalized to the first (peak) image, was then calculated. A low tail-to-peak ratio indicates better polarization. Finally, the tail-to-peak ratio was plotted against the coil currents, and a quadratic fit was added to the points. The minimum of this quadratic was taken to be the optimum current for those coils. Please note that these scans were performed when the cyclotron was ON, and the settings will not be valid when it is OFF.

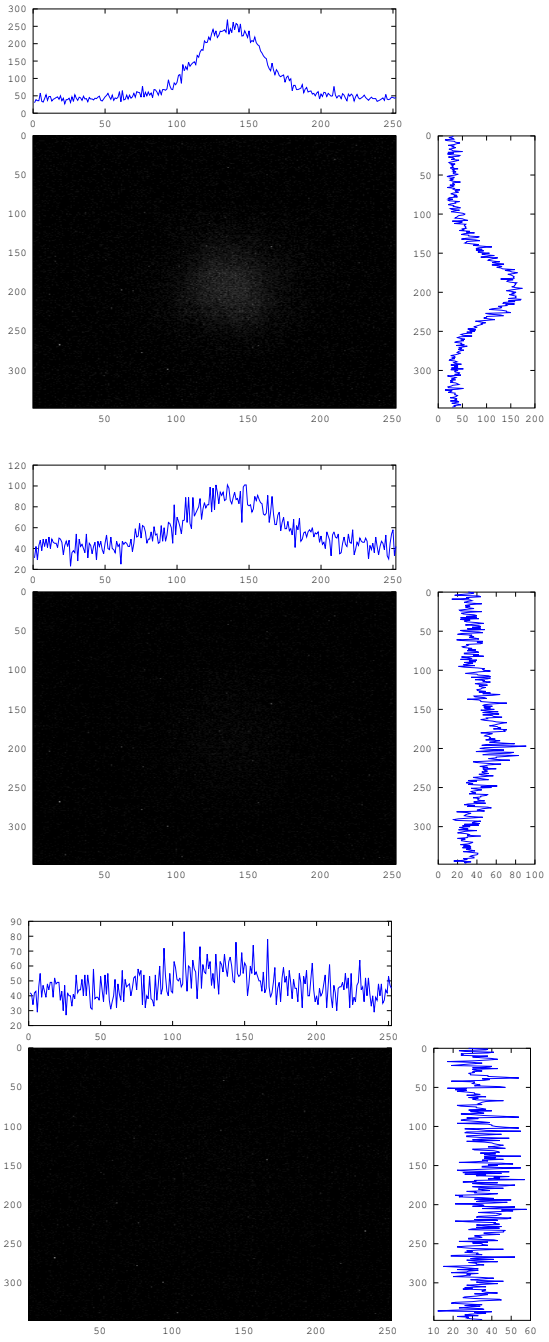

Figure 8: Example of a sequence of three optical pumping images (peak, middle and end) and their projections. This set was taken with the currents on the frame and chamber set to -0.03A and -0.02A, respectively

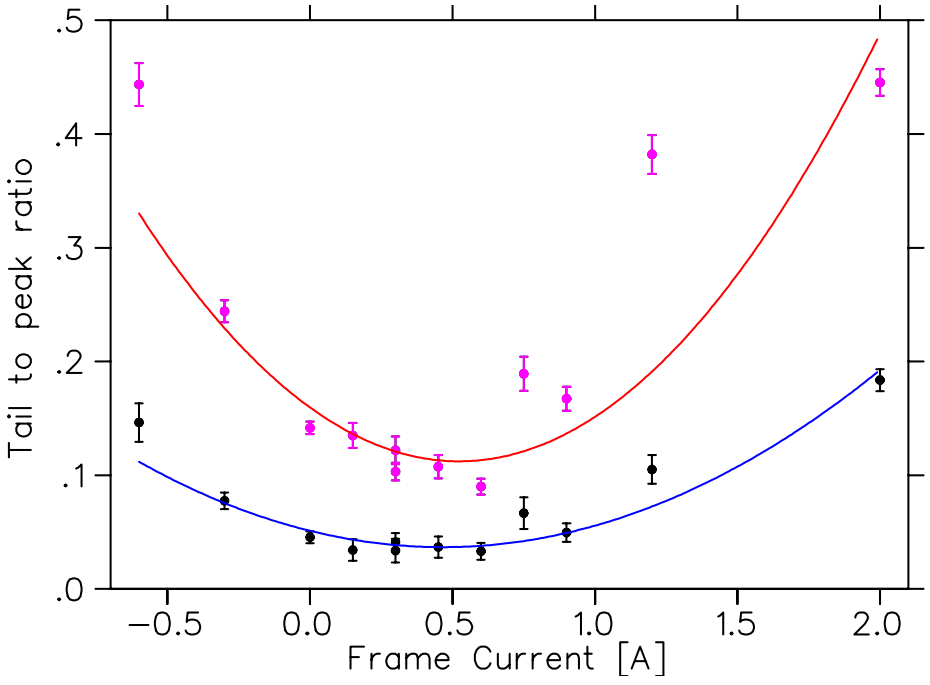

Figure 9: Tail-to-peak ratio for the frame current scan. The magenta data points and red fit represent the tail-to-peak ratio for the second optical pumping picture (OP2/OP1). The black data points and the blue fit are the tail-to-peak ratio for the third optical pumping picture (OP3/OP1). The minimum of the quadratic fit (blue) for the final optical pumping picture (OP3/OP1) represents the optimal current setting. This was found to be 0.47A ± 0.04A when the cyclotron is ON.

Frame Current Scan

For the frame coil current scan, the current was varied between +2.0A and -0.6A. The chamber current was held constant at -0.25A. The background image (pic-0) was subtracted and each image was binned into 4x4 bins to reduce noise. The resulting tail-to-peak ratios are shown in Figure 5.2 The optimum current, assumed to be the minimum of the quadratic fit for the tail-to-peak ratio for the final optical pumping image compared to the peak image, was found to be 0.47A ± 0.04A.

Chamber Current Scan

For the chamber coil current scan, the current was varied between 0.0A and -1.0A. The frame current was held constant at +0.3A. The background image (pic-0) was subtracted and each image was binned into 4x4 bins to reduce noise.

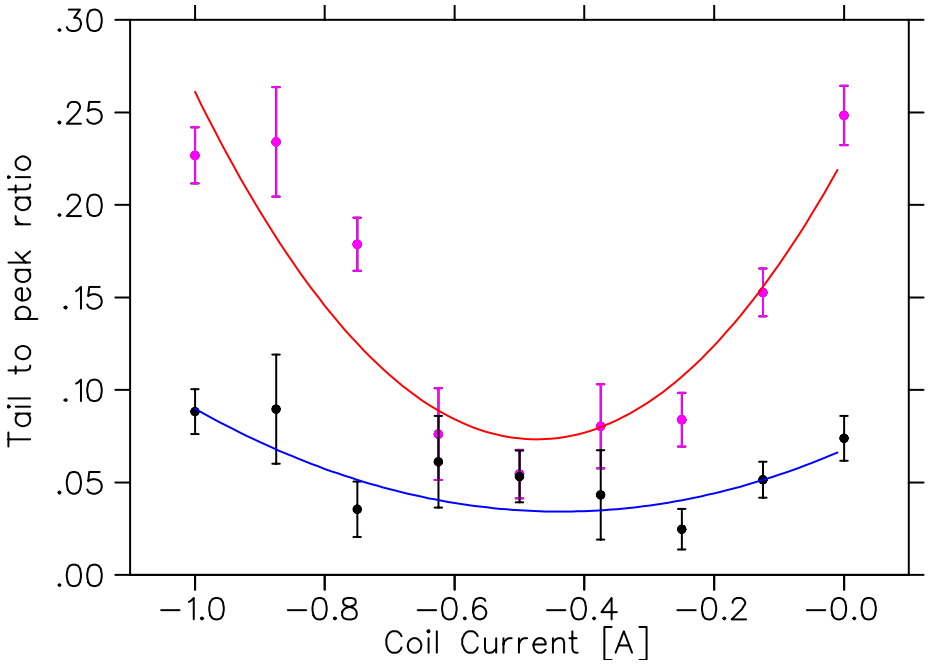

Figure 10: Tail-to-peak ratio for the coil current scan. The magenta data points and red fit represent the tail-to-peak ratio for the second optical pumping picture (OP2/OP1). The black data points and the blue fit are the tail-to-peak ratio for the third optical pumping picture (OP3/OP1). The minimum of the quadratic fit (blue) for the final optical pumping picture (OP3/OP1) represents the optimal current setting. This was found to be -0.44A ± 0.04A when the cyclotron is ON.

The resulting tail-to-peak ratios are shown in Figure 5.2. The optimum current, assumed to be the minimum of the quadratic fit for the tail-to-peak ratio for the final optical pumping image compared to the peak image, was found to be -0.44A ± 0.04A.

Linear Polarization and Holding Fields

For a frame current of +0.3A and a chamber current of -0.25A, measurements of the tail to peak ratio were performed with circular polarized light, linearly polarized light, and circularly polarized light with no holding field. The effects on the tail to peak ratio are shown in Figure 5.2 below. It can be clearly seen that the circularly polarized light produces the best tail-to-peak ratio, and that the polarization improves over the optical pumping period from the second to third pictures.

We expect the Larmor precession to depolarize the atoms at a rate of B_x^2/B_z

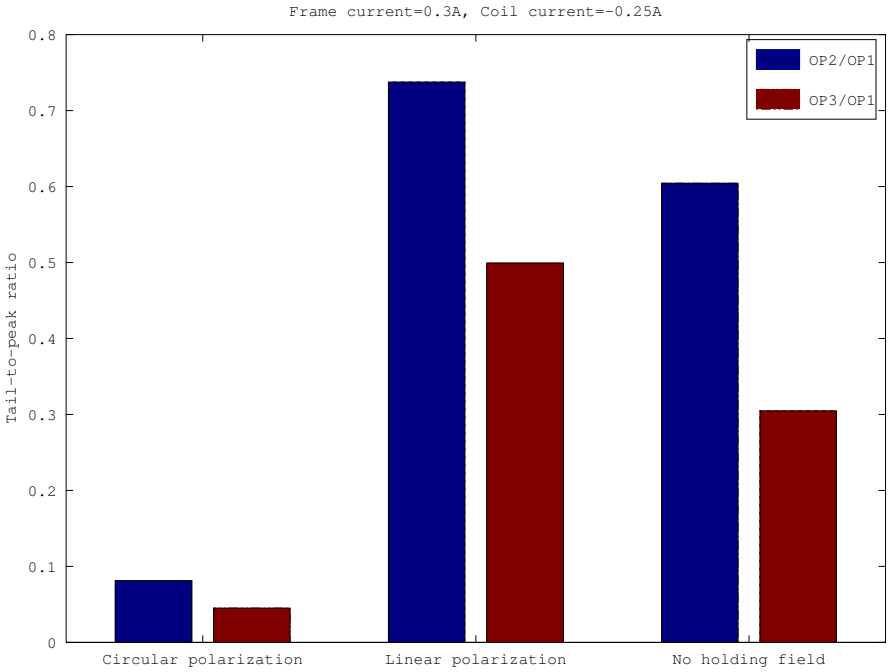

Figure 11: Tail-to-peak ratio using circularly polarized light, linearly polarized light, and circularly polarized light with no holding field. The frame current and coil current were kept at 0.3A and -0.25A, respectively, for all three sets.

where B_z is the magnetic field along the optical pumping axis and B_x is a stray transverse magnetic field. This is consistent with the quadratic functions seen in the trim field scans. It also makes sense that the holding field B_z is important to the polarization as seen in Figure 5.2. Decreasing B_z intentionally may allow for increased sensitivity when optimizing the B_x in the future.

6 Summary and Future Improvements

6.1 Summary

Over the past four months, several improvements have been made with regards to the camera imaging capabilities for the TRINAT trap. After several weeks of struggling with the old Firefly and Flea cameras, a new Grasshopper3 camera was purchased which offers low noise, global shutter, short exposure times, and good quantum efficiency in the near-IR region. After installing a new version of Point Grey's flycap software, and creating a simplified camera code drawing from several predecessors, the Grasshopper3 can now be triggered externally,

output strobes coinciding with the integration time, and write the pictures to the computer as 16-bit png images. We also implemented a new optics setup which creates a bright image signal while reducing aberrations. The optics stack also contains an interference filter which passes the optical pumping light and blocks the trap light. Several codes for Octave and Physica were created to analyze the images taken by the camera. A scan of the trim magnetic fields on the frame and on the chamber was used to optimize the current for these coils by measuring the tail-to-peak ratio for varying settings.

6.2 Recommendations

Beyond the work completed during this term, there are several topics which call for further investigation. The first is to use the Grasshopper3's imaging capabilities to optimize other settings for the trap, in a similar way to the magnetic field scans. As well, using more complex fitting routines could allow for polarization gradients within the cloud to be studied. Further integration between the Octave and Physica codes (see Appendix A) would also expediate the image analysis process and reduce the probability of human error.

In terms of the camera itself, it may be beneficial to add a support for the camera and optics stack to reduce mechanical stress and bending over the length of the lens tubes. As well, increasing the "hand-shaking" between the triggering Pi code and the camera code would allow for more confidence in the order of the image sequence, in the case of skipped images, for example. It may be possible to alter the Pi code to capture images more often, rather than the current rate of $\sim$1/second. As well, with knowledge of the strobe and timing properties, the exposure time for the photos could potentially be reduced from its current value of 200μs. The camera also has an on-board frame buffer (memory) which could be utilized for storing images before sending them to the computer.

Appendices

A Image Analysis

A.1 Image Format

The camera code is currently configured to output 16-bit greyscale .png images. The .png (portable network graphics) format is a lossless raster image format. One advantage over the text file format (.out) used in the past is that png's offer much more compression, leading to smaller file sizes. As well, because .png is a common image format, the pictures can be visually inspected with almost any image viewer. It is still possible to read .png images using a suitable program (such as Octave, see A.2) to access the numerical data for each pixel.

The .png format supports either 8-bit or 16-bit images. However, in the Grasshopper3 camera, a 12-bit ADC is used. By outputting the pictures as 16-bit images, we can take full advantage of this feature. However, the additional 4 bits do not provide any useful information and should be discarded. Due to the confusing endianness of the binary pixel values, it is easier correct the images to 12-bits once they have been read into a decimal format (where the pixel values can be divided by $2^4 = 16$ and rounded down to the nearest integer).

A.2 Octave Readout and Processing

The program GNU Octave, which is an open-source scientific programming language similar to MATLAB, was used to read and process the .png images from the camera. Octave is a suitable tool for this function because it handles arrays and matrices easily. As well, there are several built-in features which help to read and display images.

Important built-in functions

- imread: reads an image into an array of numbers, several image formats supported
- imagesc: displays an array as a scaled colour image

Custom functions

(see /trinat-blue/Documents/Erin Broatch/CustomImageEx/Most Useful Octave Codes)

- rabb.m: reads in a folder of images, adds images which occur at the same position within the trap cycle to create a single composite image (can input how many images per cycle and which position you want), corrects the images from 16-bits to 12-bits, and bins the images with a given side length

- binning.m: provides additional binning given an image and a side length for the bins
- sidwp.m: "scaled image display with projections" displays the image (colourscale based on maximum and minimum pixel values) along with the horizontal and vertical projections
- projwrite.m: makes horizontal or vertical projections for the image and outputs them to a text file, which can then be used in other applications such as fitting with Physica
- fitting functions: I experimented with some of Octave's fitting packages to fit gaussians to the image projections (projfit.m, pfwsp.m), however, they do not offer uncertainties on the fits, which is why I ended up using physica instead (see A.3)

Any of the custom functions listed above can be called in an Octave script, enabling efficient image processing. For example, the script opwrite.m uses rabb.m and binning.m to read and bin images for the optical pumping peak and two subsequent optical pumping images, generate projections and write them to text files with appropriate names.

A.3 Physica Fitting

Physica was chosen for fitting because it allows the uncertainty on fit parameters and the goodness of fit to be easily calculated. Physica can read the text files of image projections created in Octave. For example, the script opfit.pcm (located in /trinat-blue/physica/scripts) reads the projection text files produced by opwrite.m, and then fits a gaussian to each of the three composite images. The fit parameters and their uncertainties for each image are subsequently written to a text file called physicafit_outputparams.txt. The area parameter is the most important parameter for further data analysis, as it represents the brightness of the cloud. The fitting capabilities of physica were also utilized for fitting quadratics to the tail-to-peak ratios from the trim field scans (for example, the script magscan.pcm used with magquadframe.pcm and magquadchamber.pcm)

References

[1] FLIR Integrated Imaging Solutions Inc. *FLIR Machine Vision Camera Register Reference*, 4.0 edition, jan 2017.

[2] FLIR Integrated Imaging Solutions Inc. *Grasshopper3 U3 Imaging Performance Specification*, 17.2 edition, jan 2017.

[3] FLIR Integrated Imaging Solutions Inc. *Grasshopper3 U3 Technical Reference*, 18 edition, jan 2017.

[4] FLIR Integrated Imaging Solutions Inc. *Grasshopper3 USB3 Vision Datasheet*, 2017.

[5] Comar Optics. Quality planoconvex optics.

[6] Point Grey Research. *How to Evaluate Camera Sensitivity*, aug 2015.